

# CFD Investigation of 2D and 3D Dynamic Stall

**A. Spentzos, G. Barakos, K. Badcock, B. Richards  
P. Wernert<sup>+</sup>, S. Schreck<sup>++</sup>, M. Raffel<sup>+++</sup>**

<sup>+</sup> Institut de Recherche de Saint Louis, BP 34 5, Rue de l'Industrie, F-68301 SAINT LOUIS, CEDEX, France

<sup>++</sup> national renewable energy laboratory, 1617 Cole Blvd Golden, CO 80401, US

<sup>+++</sup>DLR - Institute for Aerodynamics and Flow Technology, Bunsenstr a e 10, D-37073 G ottingen, Germany

**aspentzo@aero.gla.ac.uk**  
**CFD Laboratory**  
**University of Glasgow**  
**Department of Aerospace Engineering**  
**Glasgow G12 8QQ**  
**United Kingdom**  
[www.aero.gla.ac.uk/Research/CFD](http://www.aero.gla.ac.uk/Research/CFD)

## 1 ABSTRACT

Numerical simulation has been performed for 2-D and 3-D dynamic stall cases. Square wings of NACA 0012 and NACA 0015 sections were employed and results have been compared against experimental data by Wernert *et. al.* [14] for the 2-D and Schreck and Helin [12] for the 3-D cases. The well-known flow configuration of the 2-D dynamic stall case is present on the symmetry plane of the 3-D cases. Similarities between the 2-D and 3-D cases, however, are restricted on the midspan and the flowfield changes rapidly as the wing-tip is approached. Visualisation of the 3-D calculations revealed the same omega-shaped dynamic stall vortex observed in the experiments by Schreck and Helin [12].

## 2 INTRODUCTION & LITERATURE SURVEY

Dynamic stall (DS) is known to the rotorcraft community. The phenomenon manifests itself as an augmentation of lift due to the formation of a large vortical structure over the suction side of a pitching wing. The dynamic stall vortex (DSV) is eventually shed downstream causing a sudden moment reaction and an abrupt loss of lift [10]. In the early days of DS, experimentalists attempted 3D experiments but the lack of computing power led eventually to 2D studies in order for CFD practitioners to test their codes. Although a significant amount of work has so far been performed, important information is still missing as regards 3-D and centrifugal effects.

### **Past Experimental Work on 3D DS**

A review of past experimental investigations in 3-D DS indicated that there very few cases available for validation of CFD for this complex phenomenon. A summary of the findings is presented in Table 1.

Researcher	Conditions	Measurements
Schreck & Helin	Re=6.9x10 <sup>4</sup> , M~0.1 Ramping motions	Surface pressure Flow visualisation (dye injection)
Piziali	Re=2.0x10 <sup>6</sup> , M=0.278 Ramping and oscillating motions	Surface pressure Flow visualisation (micro-tufts)
Coton & Galbraith	Re=1.5x10 <sup>6</sup> , M=0.15 Ramping and oscillating motions	Surface pressure
Tang & Dowell	Re=0.52 x 10 <sup>6</sup> , M~0.1 Oscillating motions	Surface pressure
LABM	3 x 10 <sup>5</sup> - 6 x 10 <sup>6</sup> M=0.01 - 0.3	Boundary layers Velocity profiles Turbulence quantities
Wernert <i>et al.</i>	3.73 x 10 <sup>5</sup> M~ 0.1	PIV & LSV

**Table 1: Past 3D Experimental Work**

In all cases, the experiments were conducted in the incompressible regime, with Mach number varying from 0.01 to 0.3. The geometries have been mainly NACA 0012 and NACA 0015 wings with flat or rounded tips and splitter plates on the wing root with the exception of the cases studied by Wernert [14], where he used splitter plates in both ends of the wing to ensure 2-D flow. In their work Wernert [14] have used Particle Image Velocimetry (PIV) in order to measure the precise velocity field during DS. Their results are therefore very valuable and unique as they are the only that benefit from such measurements, and they can help to study the physics of the formation and evolution of the DSV. The work undertaken by the Aerodynamics Laboratory of Marseilles (LABM) [8] employed an embedded Laser Doppler Anemometry (LDA) technique in order to provide detailed velocity measurements inside the boundary layer during DS and the experiment was designed to assist CFD practitioners with their efforts in turbulence modelling for DS. Schreck & Helin [12] were the first to provide a visual representation of the DSV (Figure 3a) using dye in a water tunnel. The researchers named the DSV observed 'Omega Vortex, due to its shape. Apart from the flow visualisation, Schreck and Helin [12] provided a detailed set of surface pressure measurements.

### Past CFD work on DS

In parallel to the experimental investigations, CFD studies have so far concentrated on 2-D DS cases. The earliest efforts to simulate DS were performed in the 70s, [10]. Initially, compressibility effects were not taken into account due to the required CPU time to perform such calculations [13]. However, in the late 90s, the problem was revisited by many researchers, [2,6,7] and issues like turbulence modelling and compressibility effects were assessed. Still, due to the lack of computing power and established CFD methods, most CFD work done until now has been focused on CFD code validation rather than the understanding of the flow physics. Barakos & Drikakis have assessed several turbulence models in their 2D study [2], stressing their importance in the accurate representation of the flow-field encountered in DS. Recently, Barakos and Drikakis [3] have presented results for an extensive range of cases and have analysed the flow configuration for the 2D case. The only 3D CFD work done to date has been performed by Ekaterinaris [6] who showed that 3D computations are possible; comparison nevertheless with experiments was very limited. The present work, therefore, is to our knowledge the first attempt to investigate the physics of the fully 3D DS phenomenon. Results are presented here for the cases by Wernert *et al.* [14] and Schreck and Helin [4] in order to highlight the differences between the 2-D and 3-D flow configurations.

### 3 CFD TOOLS

#### CFD Solver

The CFD solver used for this study is the PMB code developed at the University of Glasgow [4]. The code is capable of solving flow conditions from inviscid to laminar to fully turbulent using the Reynolds Averaged Navier-Stokes (RANS) equations in three dimensions. These equations are non-dimensionalised and transformed from a cartesian reference system to a curvilinear one before being solved. The use of the RANS form of the equations allows for fully turbulent flow conditions to be calculated with appropriate modelling of turbulence. The turbulence model used for this study has been the standard  $\kappa$ - $\omega$  turbulence model [4], however, many other turbulence models are available. To solve the RANS equations, a multi-block grid is generated around the required geometry, and the equations are discretised using the cell-centered finite volume approach. Convective fluxes are discretised using Osher's upwind scheme is used because of its robustness, accuracy and stability properties. Third order accuracy is achieved using a MUSCL interpolation technique. Viscous fluxes are discretised using central differences. Boundary conditions are set using sets of halo cells. The solution is marched implicitly in time using a second-order scheme and the final system of algebraic equations is solved using a conjugate gradient method.

#### Grid Generation

Meshing finite wings imposes a generic problem in the tip region as a single-block approach will (a) render flat tips topologically impossible and (b) lead into highly skewed cells in the case of rounded tips. For that matter two different blocking strategies were implemented as shown in Figure 1. In a first attempt (Figure 1a) the tip end is formed by an array of collapsed cells resulting in a C-H single-block topology. Although this is adequate for thin sharp tips it fails to represent the tip geometry of wings with thicker sections or flat tips. For such cases, better results can be obtained, generating a true multi-block topology (Figure 1b) where the tip constitutes one of the six sides of a new block extending to the farfield. The latter approach is capable of describing both flat and rounded tips and has been found to be more robust and accurate in the near tip region. Other approaches including H-H and C-O topologies have also been investigated.

### 4 INDICATIVE RESULTS

The aim of the present work is to compare the 2-D and 3-D flowfields and to establish the differences between the two. Starting with 2-D cases, Figure 2 compares the flowfield configurations for the case by Wernert *et al.* [14] along with the present CFD results. Three angles of attack were selected during the upstroke part of the oscillation cycle where the DSV is fully formed. The CFD calculations were performed at exactly the same conditions as the experiment, imposing a sinusoidal pitch on the blade of the form:  $\alpha=15-10\cos(kt)$  at a reduced pitch rate of  $k=0.15$ . The Reynolds number (based on the chord length) was  $3.73 \cdot 10^5$  while the Mach number was kept to  $M \sim 0.1$ . The comparison between CFD and experiments is remarkably good for this case and the DSV is predicted at the same position as the experiments indicate. Detailed comparison between CFD and the PIV data will be presented in the final paper including a detailed grid and time-convergence study carried out to guarantee the validity of the CFD predictions.

A second set of calculations is devoted to the experiment of Schreck *et al* [12]. Figure 3a presents a comparison between experiments and CFD for the fully formed omega-shaped vortex. The agreement in the overall shape is remarkable. A set of snap-shots from the CFD calculations is presented in Figure 4 where the core of the DSV and streamlines are presented. One may see that on the mid-span of the wing the flow looks like the 2D cases of Figure 2. However, as the DSV is formed, the core of the vortex stays bound to the LE region of the wing-tip while the main part of the DSV is conveyed downstream. As the DSV grows in size and its core moves above the surface of the wing, the omega-shape appears due to the fact that near the wing-tip the vortex is still bound. The phenomenon becomes more and more interesting as the tip vortex gets formed leading to a  $\Gamma - \Omega$  vortex configuration. Interestingly enough the secondary vortices formed below the DSV also appear to take the same omega shape. Further comparisons against measurements are presented in Figure 3b and 3c where  $C_p$  contours on the upper side of the wing are plotted. Overall the shape and level of the contours agrees with the measured data with the agreement getting better at higher incidence angles. The reason for this discrepancy we believe, lies in the fact that the experimentalists have used a splitter plate on the wing root with unknown surface qualities and size comparable with the DSV vortex size (the splitter plate diameter was equal to two chord lengths). Again, detailed comparisons including grid refinement and time-convergence studies have been carried out and results will be presented in the final paper.

## 5 FIGURES

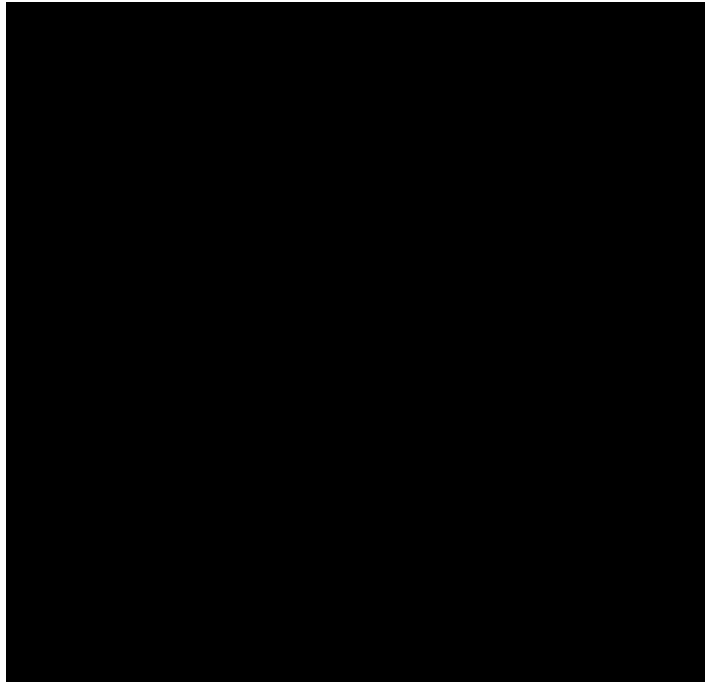


Figure 1a

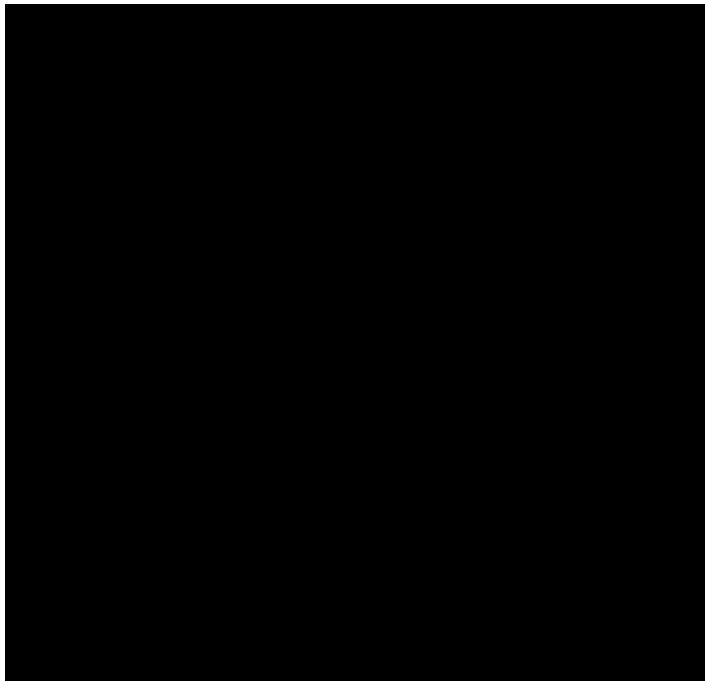


Figure 1b

**Figure 1: Topologies: a) flat tip, b) 'extruded' tip**

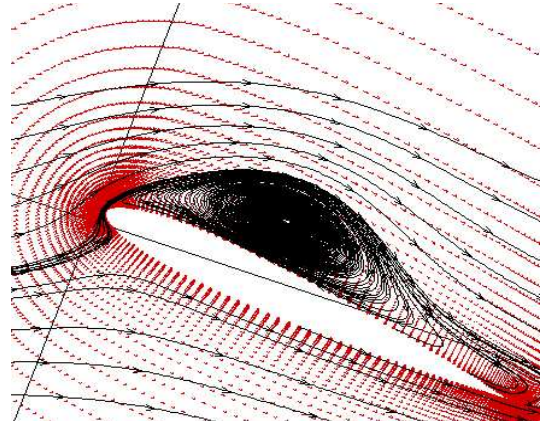
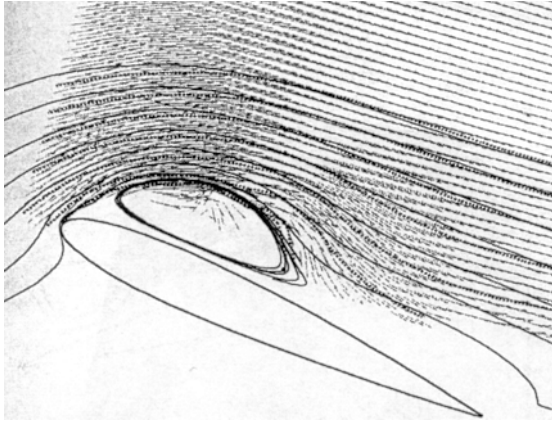


Figure 2a

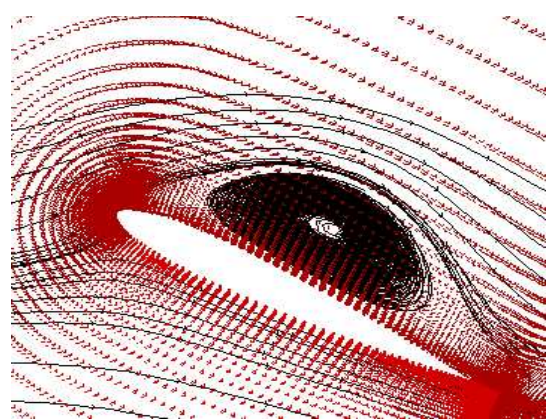
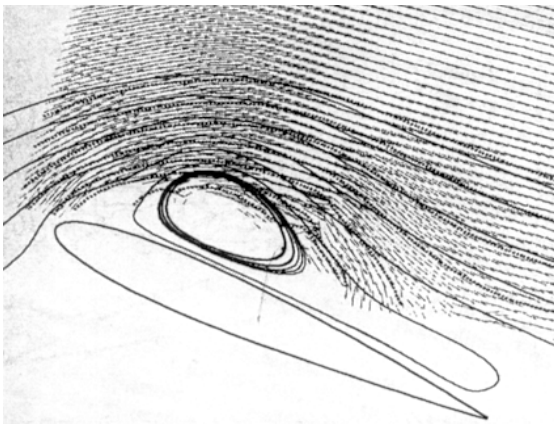


Figure 2b

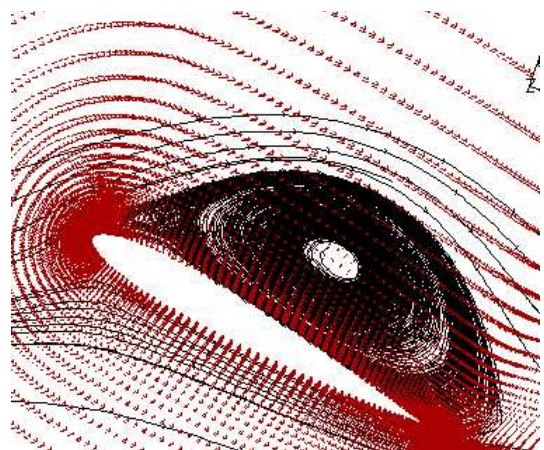
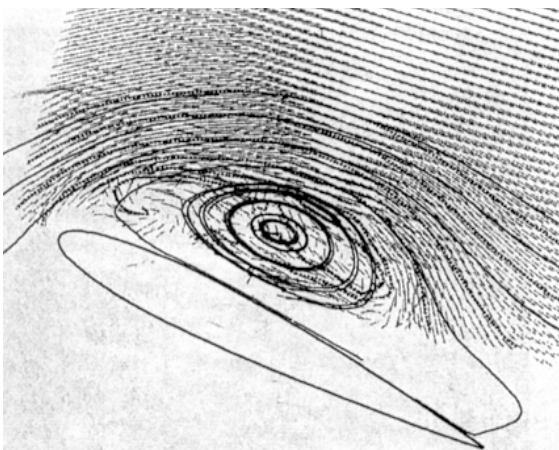


Figure 2c

**Figure 2: Comparison of CFD (right) against the experiment (left) by Wernert *et al.*  
2a) 22° upstroke, 2b) 23° upstroke and 2c) 24° upstroke**

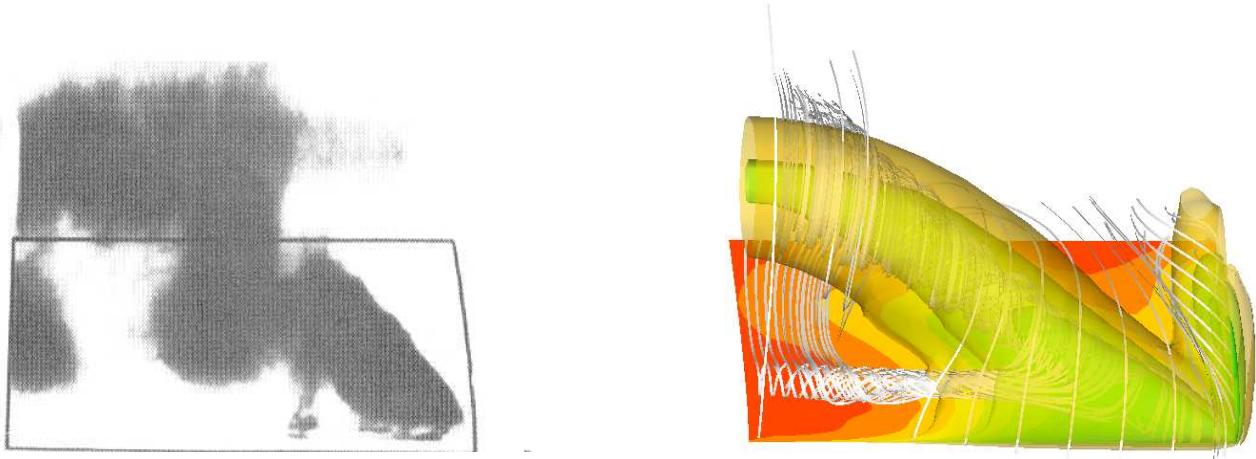


Figure 3a

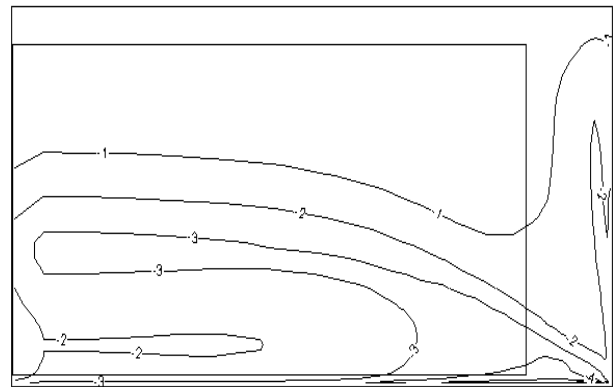
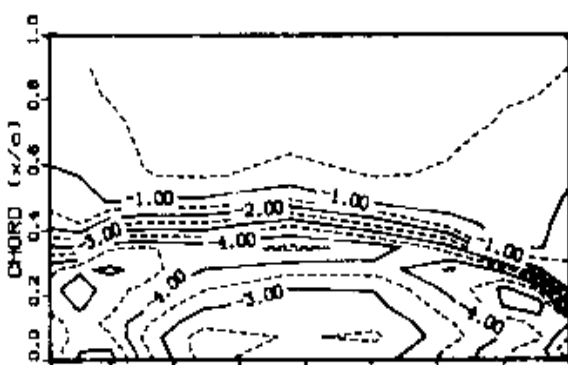


Figure 3b

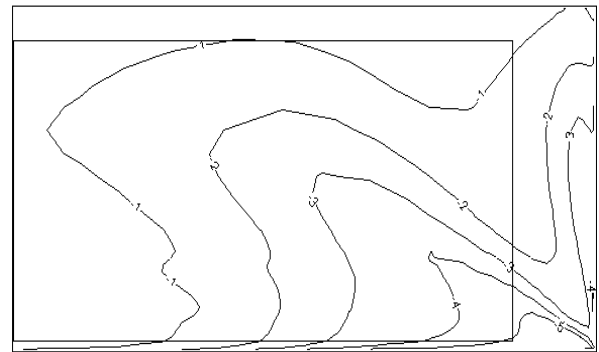
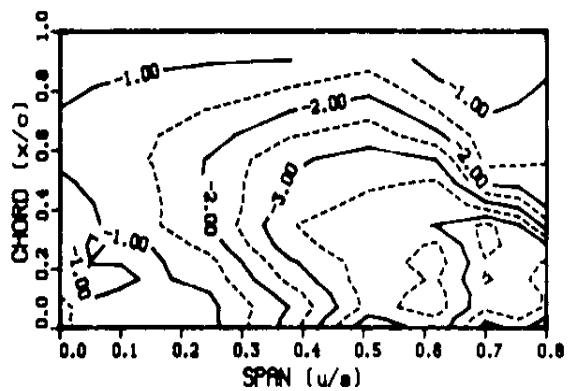


Figure 3c

Figure 3: 3a) The 'Omega' vortex as shown from the visualisations performed by Schreck & Helin (left) and the CFD representation of the same structure (right), 3b, 3c) Comparison of  $C_p$  distributions on the suction surface of the wing for AOA of 29.6 and 40.9 respectively.

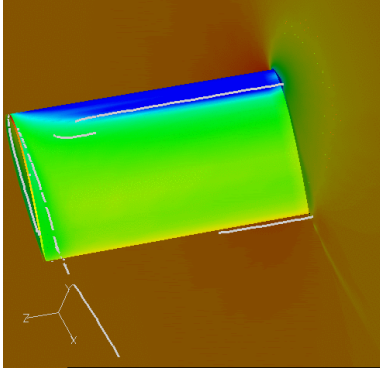


Figure 4a

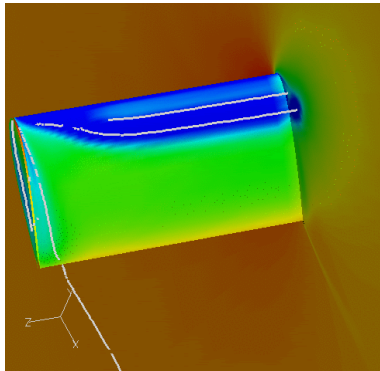
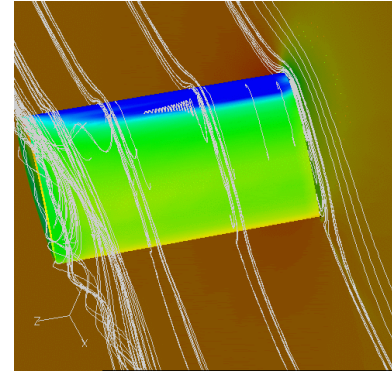


Figure 4b

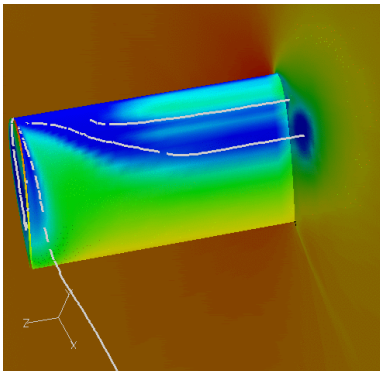
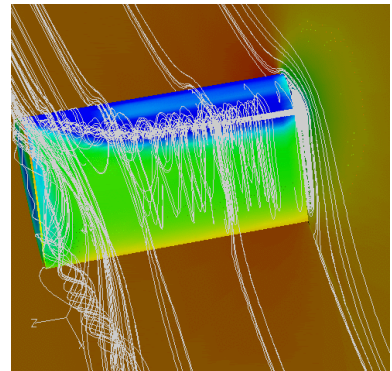


Figure 4c

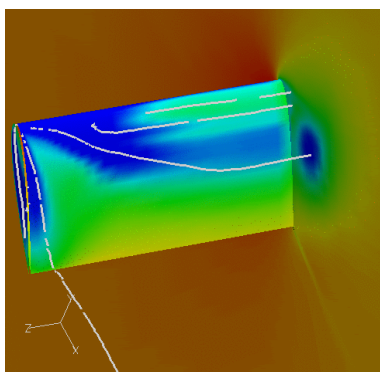
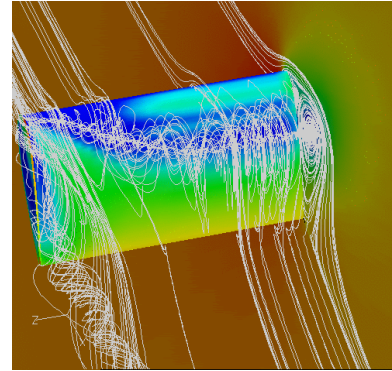
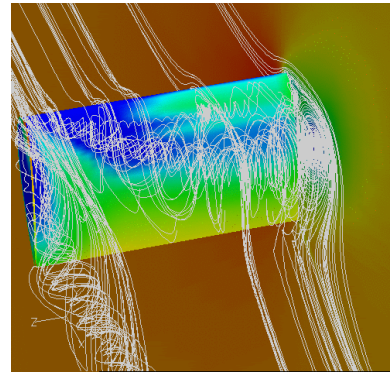


Figure 4d



**Figure 4: Vortex cores (left) and streamtraces (right) for the Schreck case, a) 13<sup>0</sup> deg, b) 20<sup>0</sup> deg, c) 25<sup>0</sup> deg and d) 28<sup>0</sup> deg**

## 8 CONCLUSIONS

Numerical simulation of the 3-D dynamic stall phenomenon has been undertaken and results have been compared against experimental data and 2-D calculations. For all cases, CFD results compared favourably against experiments. The 3-D structure of the DSV is revealed and was found to agree well with the only flow visualisation study performed so far. The evolution of the 3-D DS phenomenon was also presented. The main conclusion of this work is that similarity between 2-D and 3-D calculations is good only in the mid-span area of the wing while the outboard section is dominated by the omega-shaped vortex. The flow configuration near the wing tip is far more complex with the tip vortex and the DSV starting from the wing tip.

## 9 REFERENCES

- (1) BARAKOS G.N., and DRIKAKIS D., An Implicit Unfactored Method for Unsteady Turbulent Compressible Flows with Moving Boundaries, *Computers & Fluids*, **28**, pp 899-922, 1999
- (2) BARAKOS G.N., and DRIKAKIS D., Unsteady Separated Flows over Manoeuvring Lifting Surfaces, *Phil. Trans. R. Soc. Lond. A*, **358**, pp 3279-3291, 2000.
- (3) BARAKOS G.N., and DRIKAKIS D., Computational Study of Unsteady Turbulent Flows Around Oscillating and Ramping Aerofoils, *Int. J. Numer. Meth. Fluids*, **42**, pp 163-186, 2003
- (4) BADCOCK, K.J., RICHARDS, B.E. and WOODGATE, M.A., Elements of Computational Fluid Dynamics on Block Structured Grids Using Implicit Solvers *Progress in Aerospace Sciences*, 36, pp 351-392, 2000.
- (5) COTON F.N., GALBRAITH McD, An Experimental Study of Dynamic Stall on a Finite Wing, *The Aeronautical Journal*, **103**(1023), pp 229-236, 1999.
- (6) EKATERINARIS, J. A., Numerical Investigation of Dynamic Stall of an Oscillating Wing, *AIAA Journal*, **33**, pp 1803-1808, 1995
- (7) EKATERINARIS, J. A., *et al*, Present Capabilities of Predicting Two-Dimensional Dynamic Stall, *AGARD Conference Papers CP-552*, Aerodynamics and Aeroacoustics of Rotorcraft, August 1995
- (8) HAASE W., SELMIN V., and WINZELL B. (eds), Progress in Computational Flow-Structure Interaction, Notes on Numerical Fluid Mechanics and Multidisciplinary Design, (**81**), Springer, ISBN 3-540-43902-1
- (9) LORBER P. F., and CARTA F. O., Unsteady Stall Penetration Experiments at High Reynolds Number, *AFSOR TR-87-12002*, 1987
- (10) MCCROSKEY W.J., CARR L.W., MCALISTER K.W., Dynamic Stall Experiments on Oscillating Airfoils, *AIAA Journal* **14**(1), pp 57-63, 1976.
- (11) PIZIALI R.A., 2-D and 3-D Oscillating Wing Aerodynamics for a Range of Angles of Attack Including Stall, *NASA TM-4632*, September 1994.
- (12) SCHRECK S.J. and HELIN H.F., Unsteady Vortex Dynamics and Surface Pressure Topologies on a Finite Wing, *Journal of Aircraft*, **31**(4), pp 899-907, 1994.
- (13) VISBAL M.R., Effect of Compressibility on Dynamic Stall, *AIAA Paper* 88-0132, 1988
- (14) WERNERT P., GEISSLER W., RAFFEL M., KOMPENHANS J., Experimental and Numerical Investigations of Dynamic Stall on a Pitching Airfoil, *AIAA Journal*, **34**(5), pp 982-989, 1996.
- (15) WILCOX D.C., Reassessment of the Scale-Determining Equation for Advanced Turbulence Models, *AIAA Journal*, **26**(11), pp 1299-1310, 1988